

# Factors for increasing strength of composite materials based on fine high-calcium fly ash

Olga M. Sharonova <sup>a\*</sup> , Leonid A. Solovyov <sup>a</sup> , Alexander G. Anshits <sup>ab</sup> 

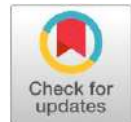
a: Institute of Chemistry and Chemical Technology SB RAS, Federal Research Center "Krasnoyarsk Science Center SB RAS", Krasnoyarsk 660036, Russia

b: Siberian Federal University, Krasnoyarsk 660041, Russia

\* Corresponding author: [shar@icct.ru](mailto:shar@icct.ru)

This paper belongs to a Regular Issue.

© 2022, the Authors. This article is published in open access under the terms and conditions of the Creative Commons Attribution (CC BY) license (<http://creativecommons.org/licenses/by/4.0/>).



## Abstract

Industrial high-calcium fly ashes obtained by burning Kansk-Achinsk coal at a thermal power plant and selected from different fields of electrostatic precipitators of an ash collecting plant were studied as the basis for composite binders (CB). The main factors influencing the properties of such CBs are the particle size, the concentration of superplasticizer at a water:binder (w/b) ratio of 0.25, and the proportion of HCFA in the mixture with cement. In particular, for cementless CBs at w/b 0.4, it was found that a change in the particle size  $d_{90}$  from 30  $\mu\text{m}$  to 10  $\mu\text{m}$  leads to an increase in compressive strength by more than 2 times – from 5.5–14 MPa to 11–36 MPa, accordingly, with a curing age of 3–300 days. The 0.12% additive of Melflux 5581F superplasticizer at w/b 0.25 increases the compressive strength – up to 14–32 MPa and up to 24–78 MPa, accordingly. The HCFA-cement blends were investigated in the range of 60–90% HCFA and the maximum compressive strength 77 MPa at 28 days of hardening was found at 80% HCFA. On the basis of 80% HCFA blend with the 0.3% addition of Melflux 5581F and 5% silica fume, the specimens of ultra-high strength (108 MPa at 28 days of hardening) were obtained.

## Keywords

binder  
high-calcium fly ash  
superplasticizer  
compressive strength  
phase composition

Received: 26.05.22

Revised: 08.07.22

Accepted: 12.07.22

Available online: 19.07.22

## 1. Introduction

Fly ash from coal burning is considered as a technogenic resource of mineral raw materials in various technologies of their processing into valuable products [1–3]. For example, because of the environmental and economic benefits, fly ashes (FAs) are used as supplementary cementitious materials (SCMs) in the production of modern construction composite materials [4–6]. The effect of fly ashes on the properties of composite materials can vary strongly depending on the fly ash composition. In the compositions with cement, all FAs exhibit a pozzolanic activity in the reaction between  $\text{Ca}(\text{OH})_2$ , which is formed during hydration of the silicate phases of cement, and aluminosilicate glass (a component of the FA) to yield calcium silicate hydrates (C–S–H), calcium aluminosilicate hydrates (C–A–S–H), and calcium aluminate hydrates (C–A–H) [7]. Fly ashes with high calcium content (20–40%) contain calcium-bearing phases that independently exhibit binding properties: lime  $\text{CaO}$ , anhydrite  $\text{CaSO}_4$ , calcium aluminate  $\text{Ca}_3\text{Al}_2\text{O}_6$ , calcium aluminoferrite

$\text{Ca}_4\text{Al}_2\text{Fe}_2\text{O}_{10}$ , and dicalcium silicate  $\beta\text{-Ca}_2\text{SiO}_4$  [8–10]. These ashes were also found to contain such crystalline phases as calcite  $\text{CaCO}_3$ , quartz  $\alpha\text{-SiO}_2$ , periclase  $\text{MgO}$ , hematite  $\alpha\text{-Fe}_2\text{O}_3$ , ferrosphenel, and various calcium aluminosilicates [11–13]. The phase composition of HCFAs varies greatly for different sources and primarily in terms of glass content: from 23 to 82% [8, 11, 12].

Moreover, the phase composition varies greatly for fly ashes sampled from different fields of electrostatic precipitators (EP).

According to the data [14], the content of the glass phase increases by 2.2 times in the series of high-calcium fly ashes from the 1<sup>st</sup> to the 4<sup>th</sup> field of the EP, but the content of free  $\text{CaO}$  decreases by a factor of 5.6. Even more radical differences are observed in the particle size, for example, the maximum size distribution shifts from ~25 to ~3  $\mu\text{m}$  for HCFA of 1<sup>st</sup> and 4<sup>th</sup> fields, respectively [8].

When the content of fine cementitious components increases in the binder, it becomes more important to use water-reducing admixtures. Already the third generation of water-reducing admixtures is used to reduce water demand

– polycarboxylate ether superplasticizers (PCE). These agents allow controlling the water-to-cement ratio and properties of fresh concrete mortar, as well as affect the hardening rate and strength of the product with high efficiency. The mechanism of action of PCE is based on the fact that carboxyl groups ( $-\text{COOH}$ ) in the polymer backbone ensure adsorption on the surface of cement grains, while side polyester chains cause steric hindrance, thus preventing the coalescence of fine particles [15]. Different components of the mineralogical composition of cement are known to vary in terms of their adsorption characteristics with respect to superplasticizers. Namely, calcium silicates  $\text{Ca}_3\text{SiO}_5$  and  $\text{Ca}_2\text{SiO}_4$  have a negative  $\zeta$ -potential ( $-5$  mV), while calcium aluminate  $\text{Ca}_3\text{Al}_2\text{O}_6$  and calcium aluminoferrite  $\text{Ca}_4\text{Al}_2\text{Fe}_2\text{O}_{10}$  are characterized by a positive  $\zeta$ -potential ( $\sim +10$  and  $+5$  mV, respectively) [16]. Once the superplasticizer is adsorbed, the surface of  $\text{Ca}_3\text{Al}_2\text{O}_6$  and  $\text{Ca}_4\text{Al}_2\text{Fe}_2\text{O}_{10}$  becomes negatively charged, thus contributing to mutual repulsion of cement particles and causing high dispersibility of cement. There are few data on the behavior of dispersed mineral components with respect to superplasticizers in the available literature. So, for example, the study focused on cements with admixtures of aluminosilicate FA, ground limestone powder, and blast-furnace slag with  $\zeta$ -potentials of  $+13$  mV,  $+2.5$  mV, and  $-2.7$  mV, respectively, showed that the greatest amount of polycarboxylate ether superplasticizer was adsorbed in the case of limestone powder, while this amount was the lowest in the case of slag [17]. Therefore, in order to achieve identical rheological parameters, the highest superplasticizer concentration was used in the case of limestone powder, and the lowest superplasticizer concentration, in the case of slag admixture.

Although the scope of practical application of coal ashes is currently expanding, there is still no clear understanding of the regularities of the influence of the composition, the particle size, as well as the type and concentration of a superplasticizer, on the structure and properties of cementitious materials based on fly ash, in particular, on high-calcium fly ash. This study aimed to investigate the influence of the particle size, the composition of HCFA and HCFA-PC blends, as well as the content of a superplasticizer admixture on the strength properties of cement-free and highly filled (60–90% HCFA) composite cements materials.

## 2. Experimental

### 2.1. Objects

High-calcium fly ashes produced during pulverized combustion of grade B2 low-ash (11%) brown coal mined from the Kansk–Achinsk coal basin were used as the starting material for the composite specimens. The coal was burned at a temperature of  $1400\text{--}1500$  °C in the furnaces of the BKZ-420 boiler with liquid slag removal at the Krasnoyarsk Thermal Power Plant 2. The fly ashes were

sampled from fields 3 and 4 of electrostatic precipitators (fractions 3 and 4, respectively) on a setup characterized by a particle capture efficiency of  $\geq 98\%$ . Portland cement PC 42.5 N manufactured at Krasnoyarsk Cement Plant was also used in this study. Melflux 5581F polycarboxylate ether superplasticizer (BASF Construction Solutions, Trostberg, Germany) and silica fume MKU-95 (Stromex OJSC, Moscow, Russia) were used as admixtures.

### 2.2. Methods

Particle size distribution was measured on an Analysette 22 MicroTec laser diffraction particle size analyzer (Fritsch, Germany) using a dry cell. The macrocomponent composition ( $\text{SiO}_2$ ,  $\text{Al}_2\text{O}_3$ ,  $\text{Fe}_2\text{O}_3$ ,  $\text{CaO}$ ,  $\text{MgO}$ ,  $\text{SO}_3$ ,  $\text{Na}_2\text{O}$ ,  $\text{K}_2\text{O}$ , and  $\text{TiO}_2$ ) and loss on ignition (LOI) were determined by chemical analysis in compliance with a State standard GOST 5382-91.

Quantitative XRD analysis was performed using the full-profile Rietveld method [18]. The XRD patterns were recorded in reflection geometry using  $\text{Co K}\alpha$  radiation on a PANalytical X'Pert PRO diffractometer equipped with a PIXcel detector and a graphite monochromator. The XRD pattern were recorded in the range of diffraction angles  $2\theta=7\text{--}100^\circ$ . The mass percentages of the crystalline and amorphous components were determined by the external standard method (using corundum). The absorption coefficients of the samples were calculated from the total elemental composition according to the chemical analysis data. This method has been successfully used for quantification of the phase composition of HCFA [8, 10]. The specific surface area (SSA) was determined using a NOVA 3200e sorption analyzer (Quantachrome Instruments, USA) in the low-temperature nitrogen adsorption/desorption mode at  $-195.8$  °C ( $77.35$  K) in the range of relative pressures  $P/P_0=0.01\text{--}0.995$ .

The  $20\times 20\times 20$  mm hardened cube-shaped composite specimens were produced from 100% HCFA (fraction 3 or 4) at a water–binder ratio  $w/b = 0.4$  without the superplasticizer (specimens FA-3 and FA-4, respectively) or at a water–binder ratio  $w/b = 0.25$  with an admixture of 0.12 wt.% Melflux 5581F superplasticizer (specimens 100fa-3 and 100fa-4, respectively). Superplasticizer concentration was chosen according to the results of the flowability test [10]. The reference specimens were produced from cement PC 42.5 N at a  $w/b$  ratio = 0.4 without a superplasticizer (specimen PC\_04) and  $w/b = 0.25$  with the admixture of 0.12 wt.% Melflux 5581F superplasticizer (specimen PC\_025). All the specimens were stored in a moist atmosphere for 1–300 days. The specimens of the composite materials with composition HCFA–PC were prepared (where HCFA is fraction 4, its content in the blend being 60, 70, 80 and 90%) at  $w/b = 0.25$  and concentration of the Melflux 5581F superplasticizer being 0.12% (specimens 60fa, 70fa, 80fa, and 90fa, respectively). The composition containing 80% HCFA was used to produce the specimen 80fa-SF at  $w/b$  ratio = 0.25 with an admix-

ture of 0.3% Melflux 5581F superplasticizer and 5% of silica fume to the blend. The strength tests of the specimens were conducted on a 3360 Series dual column tabletop universal testing system (Instron, USA) at a frame speed of 5 mm/min. Compressive strength was measured for four cubes for each curing age, and calculated as the average of three nearest strength values.

### 3. Results and discussion

#### 3.1. Characteristics of initial fractions of HCFA and Portland cement

The particle size distribution data (Table 1) show that HCFA fraction 4 has a much smaller particle size compared to that of fraction 3. In particular,  $d_{90}$  is ~10 and 30  $\mu\text{m}$ , while  $d_{50}$  is 4 and 9  $\mu\text{m}$  for fractions 4 and 3, respectively. Meanwhile, both these fractions are much smaller than PC particles. For PC 42.5 N, the particle size distribution is shifted towards coarser particles:  $d_{90}$  and  $d_{50}$  are 55 and 20  $\mu\text{m}$ , respectively. The total specific surface area (SSA) of powder materials is primarily determined by the particle size, but it is also influenced by other factors such as particle density and porosity.

The studied HCFA fractions consist of microspheres of different sizes and morphologies [14]. The microspheres are formed from authigenic minerals (being responsible for their composition) contained in coal in the porous structure of the carbon matrix regulating their size [19].

The analyzed fractions 3 and 4 sampled from fields 3 and 4 of the electrostatic precipitators of the ash collection facility have similar chemical compositions, as can be seen from the content of the five main components of the composition (Figure 1). The predominant component is CaO (40 and 39.69 wt.%); the content of  $\text{SiO}_2$  is appreciably high (24.26 and 24.60 wt.%), while the content of other macrocomponents is significantly lower ( $\text{Al}_2\text{O}_3$ , 6.71 wt.% and 7.30 wt.%;  $\text{Fe}_2\text{O}_3$ , 13.45 wt.% and 14.29 wt.%; MgO, 9.10 wt.% and 8.24 wt.%, respectively). Unlike Portland cement PC 42.5 N, these fractions are characterized by a lower (1.6-fold) content of CaO, but higher contents of the  $\text{SiO}_2$ ,  $\text{Al}_2\text{O}_3$ ,  $\text{Fe}_2\text{O}_3$ , MgO components. Both fractions are characterized by a significantly higher content of total CaO compared to most Class C fly ashes from pulverized coal combustion [1, 20–22], which causes a higher contribution of Ca-containing phases.

Fractions 3 and 4 contain the same phases, but there are some differences in their contents. The amorphous phase (32.6 and 42.1 wt.%) is the predominant component of both fractions 3 and 4 [14].

**Table 1** Dispersity characteristics of HCFA fractions 3 and 4 and Portland cement PC 42.5 N.

Sample	$d_{90}$ , $\mu\text{m}$	$d_{50}$ , $\mu\text{m}$	SSA, $\text{g}/\text{cm}^3$
Fraction 3	30	9	1.52
Fraction 4	10	4	2.36
PC 42.5 N	55	20	0.30

Fraction 4 is characterized by lower contents of the  $\text{Ca}_3\text{Al}_2\text{O}_6$  and CaO phases, while the contents of  $\text{Ca}_2\text{Fe}_x\text{Al}_y\text{O}_5$ ,  $\text{CaCO}_3$ ,  $\text{Ca}(\text{OH})_2$  and the amorphous phase are increased.

In comparison with the fly ash fractions, PC 42.5 N cement has a qualitatively different phase composition [14]. It contains tricalcium silicate  $\text{Ca}_3\text{SiO}_4$  as the predominant component (64.5 wt.%), and clinker phases typical of cement are also present: dicalcium silicate  $\text{Ca}_2\text{SiO}_4$ , aluminoferrite  $\text{Ca}_2\text{Fe}_x\text{Al}_y\text{O}_5$ , aluminate  $\text{Ca}_3\text{Al}_2\text{O}_6$ , as well as calcium sulfate hydrates  $\text{CaSO}_4 \cdot 0.5\text{H}_2\text{O}$  and  $\text{CaSO}_4 \cdot 2\text{H}_2\text{O}$ , which are commonly added during grinding.

#### 3.2. The effect of particle size of HCFA fractions on strength of composite materials without and with superplasticizer admixture

A detailed description of the prepared composite specimens is given in Table 2.

Measuring compressive strength ( $\sigma_{\text{comp}}$ ) of the specimens based on 100% HCFA of each fraction 3 and 4 at a water-binder ratio  $w/b = 0.4$  without a superplasticizer (Figure 2, specimens FA-3 and FA-4) demonstrated that  $\sigma_{\text{comp}}$  is 2- to 2.6-fold higher for FA-4 compared to FA-3 and is equal to 11–36 MPa and 5.5–14 MPa, respectively, at the curing age of 3–300 days.

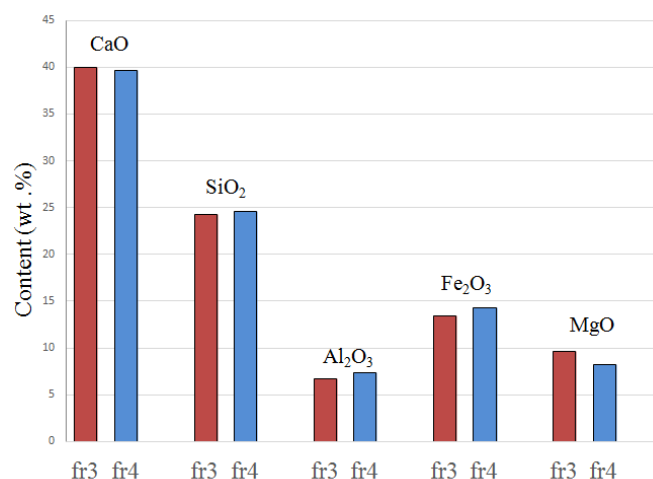


**Figure 1** The content of the main components in the chemical composition of fractions 3 and 4.

**Table 2** Mixture proportion (wt. %) of composite materials (SF – silica fume; W/B – water/binder ratio; SP – superplasticizer).

Specimen	HCFA		PC	SF	W/B	SP
	Fr. 3	Fr. 4				
FA-3	100	–	–	–	0.4	–
FA-4	–	100	–	–	0.4	–
PC_04	–	–	100	–	0.4	–
PC_025	–	–	100	–	0.25	0.12
100fa-3	100	–	–	–	0.25	0.12
100fa-4	–	100	–	–	0.25	0.12
60fa	–	60	40	–	0.25	0.12
70fa	–	70	30	–	0.25	0.12
80fa	–	80	20	–	0.25	0.12
90fa	–	90	10	–	0.25	0.12
80fa-SF	–	80	20	5	0.25	0.3

While the fractions' compositions differ only slightly, the higher fineness of fraction 4 is the key factor being responsible for the higher strength of the FA-4 specimens compared to those of the FA-3 specimens. The most active phases of these HCFA are  $\text{Ca}_2\text{Fe}_x\text{Al}_y\text{O}_5$ ,  $\text{CaSO}_4$ ,  $\text{CaO}$  and glass [10] more actively involved in the hydration process with an increase in the dispersion of the ash material, forming more hydrate products that increase strength.

The effect of fraction fineness on the strength of composite materials is quite expected when using the Melflux 5581 F superplasticizer, which provides better dispersibility of micron and submicron particles in the liquid phase. Melflux 5581F is a polycarboxylate ether superplasticizer consisting of the poly(methacrylic acid) backbone and methoxypolyethylene glycol side chains [23]. The mechanism of dispersion ensured by Melflux 5581F superplasticizer is considered to be related to electrostatic repulsive forces generated by carboxyl groups ( $-\text{COO}^-$ ) of the backbone on the surface of cement grains and to the steric effect of repulsion induced by the hydrophobic side chains of methoxypolyethylene glycol [24]. The effect of superplasticizer admixture was studied for the specimens based on 100% HCFA of each fraction (3 and 4) at Melflux 5581F concentration of 0.12% and w/b ratio = 0.25 (Figure 3, specimens 100fa-3 and 100fa-4, respectively).

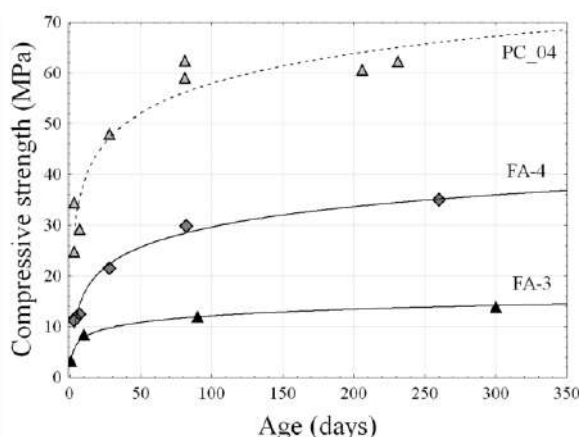


**Figure 2** Compressive strength of specimens FA-3 and FA-4 and Portland cement PC\_04 at a w/b ratio = 0.4 without superplasticizer added.

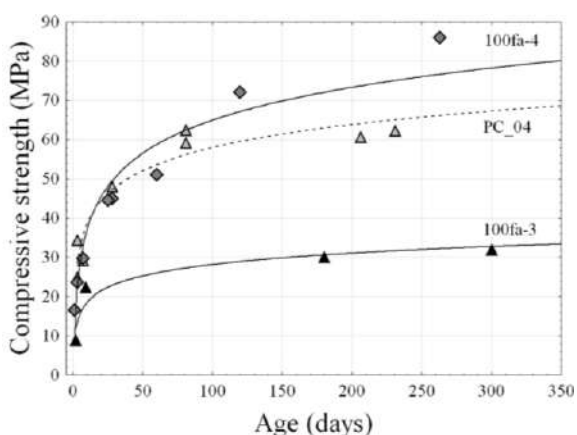


**Figure 3** Compressive strength of specimens 100fa-3 and 100fa-4 at a w/b ratio = 0.25 with an admixture of 0.12% Melflux 5581F and PC\_04 at a w/b ratio = 0.4 in the absence of superplasticizer.

The findings indicate that strength of 100fa-4 specimens increased more than two-fold: up to 24–78 MPa after the curing age of 3–300 days. A similar effect was also observed for 100fa-3 specimens, whose strength increased to 14–32 MPa after the same curing age. The  $\sigma_{\text{comp}}$  value of 100fa-4 specimens was similar to that of the reference specimens based on Portland cement PC 42.5 N at w/b ratio = 0.4 without the superplasticizer (PC\_04) during the early curing age, while being higher than that of the reference specimen by ~10 MPa during the late curing age (Figure 3). More detailed studies were conducted for the specimens based on fraction 4.

### 3.3. The effect of cement admixtures on strength of composite materials

The effect of cement admixtures on activity of the fly ash fraction 4 was studied for the specimens of composite materials based on mixture HCFA-PC (Table 2), where the PC content is 10, 20, 30, and 40% and the HCFA is fraction 4 with its content in the blend of 90, 80, 70, and 60 wt.% (specimens 90fa; 80fa; 70fa, and 60fa, respectively). Strength values of the specimens containing an admixture of 40 wt.% cement (specimen 60fa) and the without cement admixture (specimen 100fa-4) at the curing age of 28 days are comparable to those of specimen PC\_04 based on 100 wt.% cement at w/b ratio = 0.4 in the absence of superplasticizer (Figure 4). If the content of cement admixture is 10–30 wt.% (HCFA content is 70–90 wt.%), the compressive strength rises and passes through the maximum at PC content of 20 wt.% (specimen 80fa in Figure 4), where  $\sigma_{\text{comp}}$  is 77 and 125 MPa at the curing age 28 and 100 days, respectively.

With an increase in curing age to 100 days, the strength of specimens with a high fly ash content (specimens 70fa, 80fa, 90fa, and 100fa4) increases to a greater extent (1.3–1.6 times) compared to specimens with a high cement content (PC\_04, 60fa, PC\_025), for which the strength increases by 1.1–1.16 times (Figure 4). The observed rise in strength is the significant advantage of using fine HCFA as a basis for cementitious composite materials.

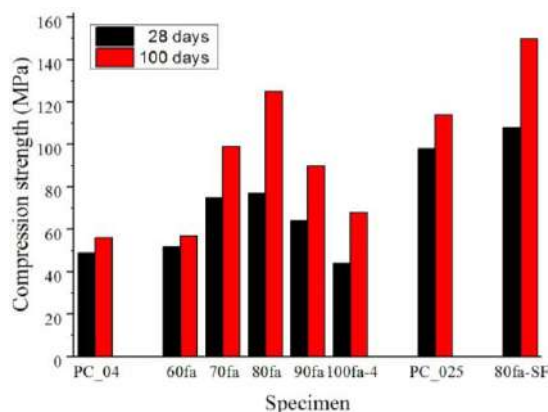


**Figure 4** Compressive strength of the composite specimens based on PC 42.5 N (PC\_04 and PC\_025), on fraction 4 (100fa-4), on HCFA-PC blends (60fa, 70fa, 80fa, and 90fa), and sample 80fa-SF containing 0.3% Melflux 5581F and 5% of silica fume added to the blend.



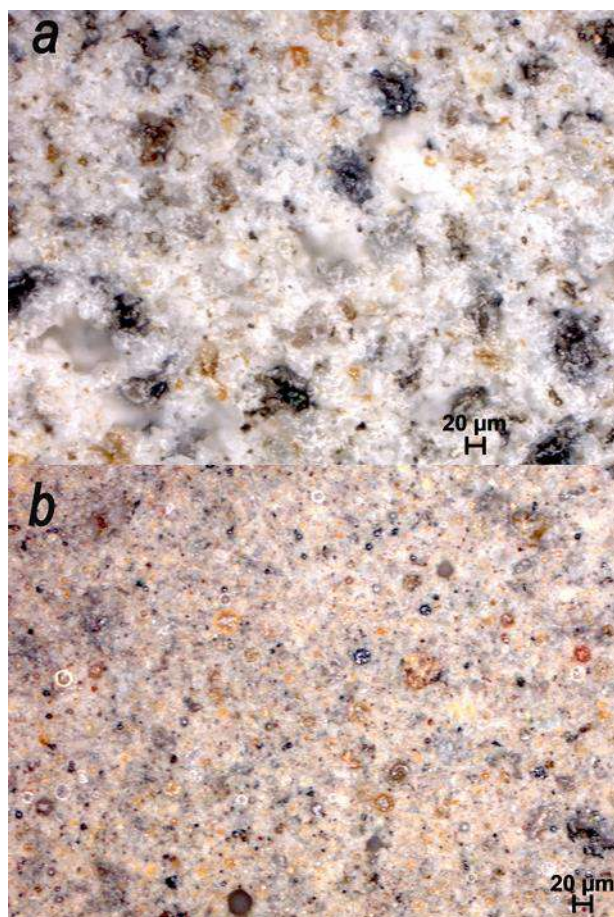


**Figure 5** Optical microscope images of the cured specimens at 100 days: Portland cement (a); 80% fr4 - 20% PC (b).

A similar effect was observed by the authors of [4] when 18% of PC was replaced with Class C fly ash (CaO 36.56 wt.%) in self-consolidating concretes containing a polycarboxylate ether superplasticizer HRWR (admixture content, 1.28 wt.%). The specimens were obtained with a compressive strength close to that of specimens based 100 wt.% PC at curing age of 7 days and exceeding it by 3–6 MPa at the curing age of 28–90 days. As the ash content increased to 36%, the strength increased even more. Unlike high-calcium fly ash, admixtures of fly ash with aluminosilicate composition (Class F) usually reduce early strength of cement-based composite materials [4, 25]. For example, the addition of Class F fly ash of 10–40% leads to a decrease in strength by 1.5–3 times at the curing age of 3–7 days and, with an increase to 70% FA, the strength decreased by 6–13 times. Thus, the factors for improving the strength of cement compositions in the early stages are the higher CaO content in fly ash, the decrease in the size of ash particles, and the addition of a superplasticizer, which facilitates their dispersion.

It was previously established [14] that the main newly formed phases for the binder based 100% HCFA are ettringite  $3\text{CaO}\cdot\text{Al}_2\text{O}_3\cdot 3\text{CaSO}_4\cdot 32\text{H}_2\text{O}$ , calcium carboaluminate hydrates  $\text{Ca}_4\text{Al}_2(\text{OH})_{13}(\text{CO}_3)_{0.5}\cdot 4\text{H}_2\text{O}$ ,  $\text{Ca}_4\text{Al}_2(\text{OH})_{12}\text{CO}_3\cdot 5\text{H}_2\text{O}$  and cryptocrystalline calcium hydrosilicates. Since calcium aluminoferrite  $\text{Ca}_2\text{Fe}_x\text{Al}_y\text{O}_5$  was actively involved in their formation, the ettringite and

calcium carboaluminate phases are solid solutions due to the isomorphous replacement of  $\text{Al}^{3+}$  with  $\text{Fe}^{3+}$ . The main source of silicates is the amorphous phase (glass). The contribution of glass transformation yielding cryptocrystalline calcium hydrosilicates increases with curing time.

The microstructure of the hardened sample obtained with the addition of HCFA fraction 4 (Figure 5) becomes thinner compared to the hardened Portland cement sample and, consequently, finely mixed hydrate phases are formed, providing a higher strength of the composite material.

Based on a blend of 80% HCFA - 20% PC at  $w/b = 0.25$ , the ultra-high strength specimens (80fa-SF) were obtained by increasing the concentration of Melflux 5581F to 0.3% and adding silica fume (SF) in an amount of 5%. Compressive strength of 80fa-SF specimens is 108 and 150 MPa at curing age 28 and 100 days, respectively (Figure 4). Adding the silica fume can improve properties of composite materials due to denser packing of particles and the pozzolanic reaction with  $\text{Ca}(\text{OH})_2$  yielding additional calcium hydrosilicates [15].

#### 4. Conclusions

The factors of improving the strength of the composite materials based on high-calcium fly ash were investigated in this study.

The effect of particle fineness on strength of the cementless composite materials based on microspherical fractions of high-calcium fly ashes (HCFA) with total CaO content of ~40 wt.% was studied. It was found that for fly ash fractions having similar chemical and phase compositions, a decrease in the particle size from  $d_{90}$  30  $\mu\text{m}$  (fraction 3) to 10  $\mu\text{m}$  (fraction 4) increases compressive strength more than twofold: from 5.5–14 MPa to 11–36 MPa at curing age of 3–300 days.

The effect of adding a superplasticizer was studied and it was found that the addition of 0.12% Melflux 5581F made it possible to reduce the  $w/b$  ratio to 0.25 and increase the strength by 2.3–2.5 times for the specimens based on fraction 3 - up to 14–32 MPa and by 2.2 times for the specimens based on fraction 4 - up to 24–78 MPa at the curing age of 3–300 days.

The influence of adding PC 42.5 N on the enhancement of strength of the composite materials based on HCFA fraction 4 of in the presence of 0.12% Melflux 5581F at  $w/b$  ratio = 0.25 was studied in the range of 10–40% PC. It was found that the value of compressive strength has a maximum at 20% PC (80% HCFA), which is 77 and 125 MPa with the curing age of 28 and 100 days, respectively.

On the basis of the composition 80%HCFA-20%PC, the ultra-high strength specimens were obtained with the addition of 0.3% Melflux 5581F and 5% silica fume, which have a compressive strength of 108 and 150 MPa at the curing age of 28 and 100 days, respectively.

## Supplementary materials

No supplementary data are available.

## Funding

This work was conducted within the framework of the budget project No. 121031500198-3 for Institute of Chemistry and Chemical Technology SB RAS.

## Acknowledgments

This work was conducted using the equipment of Krasnoyarsk Regional Research Equipment Centre of SB RAS. The authors are grateful to E.V. Mazurova for obtaining SEM images.

## Author contributions

Conceptualization: O.M.S., A.G.A.

Data curation: O.M.S.

Formal Analysis: O.M.S., L.A.S., A.G.A.

Funding acquisition: O.M.S., L.A.S., A.G.A.

Investigation: O.M.S., L.A.S., A.G.A.

Methodology: O.M.S., L.A.S., A.G.A.

Project administration: A.G.A.

Resources: O.M.S., L.A.S., A.G.A.

Software: O.M.S., L.A.S.

Supervision: A.G.A.

Validation: O.M.S., A.G.A.

Visualization: O.M.S., L.A.S., A.G.A.

Writing – original draft: O.M.S., A.G.A.

Writing – review & editing: O.M.S.

## Conflict of interest

The authors declare no conflict of interest.

## Additional information

Author IDs:

Olga M. Sharonova, Scopus ID [650611906](https://orcid.org/0009-0001-6506-11906);

Leonide A. Solovyov, Scopus ID [6701367459](https://orcid.org/0009-0001-6701-367459);

Alexander G. Anshits, Scopus ID [57200009289](https://orcid.org/0009-0001-5720-0009289).

Websites:

Institute of Chemistry and Chemical Technology SB RAS, Federal Research Center "Krasnoyarsk Science Center SB RAS", <https://ksc.krasn.ru>;

Siberian Federal University, <https://www.sfu-kras.ru>.

## References

- Blissett RS, Rowson NA. A review of the multi-component utilisation of coal fly ash. *Fuel*. 2012;97:1–23. doi:[10.1016/j.fuel.2012.03.024](https://doi.org/10.1016/j.fuel.2012.03.024)
- Belviso C. State-of-the-art applications of fly ash from coal and biomass: A focus on zeolite synthesis processes and issue. *Prog Energy Comb Sci*. 2018;5:109–135. doi:[10.1016/j.pecs.2017.10.004](https://doi.org/10.1016/j.pecs.2017.10.004)
- Snegirev VA, Yurk VM. The development of technology for production of zeolites from fly-ash from Troitskaya power plant. *Chimi Techno Acta*. 2021;8:20218111. doi:[10.15826/chimtech.2021.8.1.11](https://doi.org/10.15826/chimtech.2021.8.1.11)
- Ahari RS, Erdem TK, Ramyar K. Permeability properties of self-consolidating concrete containing various supplementary cementitious materials. *Constr Build Mater*. 2015;79:326–336. doi:[10.1016/j.conbuildmat.2015.01.053](https://doi.org/10.1016/j.conbuildmat.2015.01.053)
- Pranav S, Aggarwal S, Yang E-H, Sarkar AK, Singh AP, Lahoti M. Alternative materials for wearing course of concrete pavements: A critical review. *Constr Build Mater*. 2020;236:117609. doi:[10.1016/j.conbuildmat.2019.117609](https://doi.org/10.1016/j.conbuildmat.2019.117609)
- Rahul AV, Santhanam M, Meena H, Ghani Z. Mechanical characterization of 3D printable concrete. *Constr Build Mater*. 2019;227:116710. doi:[10.1016/j.conbuildmat.2019.116710](https://doi.org/10.1016/j.conbuildmat.2019.116710)
- Donatello S, Fernández-Jimenez A, Palomo A. Very high volume fly ash cements. Early age hydration study using Na<sub>2</sub>SO<sub>4</sub> as an activator. *J Am Ceram Soc*. 2013;96:900–906. doi:[10.1111/jace.12178](https://doi.org/10.1111/jace.12178)
- Sharonova OM, Solovyov LA, Oreshkina NA, Yumashev VV, Anshits AG. Composition of high-calcium fly ash middlings selectively sampled from ash collection facility and prospect of their utilization as component of cementing materials. *Fuel Process Technol*. 2010;91:573–581. doi:[10.1016/j.fuproc.2010.01.003](https://doi.org/10.1016/j.fuproc.2010.01.003)
- Zhao Y, Zhang J, Tian C, Li H, Shao X, Zheng C. Mineralogy and chemical composition of high-calcium fly ashes and density fractions from a coal-fired power plant in China. *Energy Fuels*. 2010;24:834–843. doi:[10.1021/ef900947y](https://doi.org/10.1021/ef900947y)
- Sharonova OM, Kirilets VM, Yumashev VV, Solovyov LA, Anshits AG. Phase composition of high strength binding material based on fine microspherical high-calcium fly ash. *Constr Build Mater*. 2019;216:525–530. doi:[10.1016/j.conbuildmat.2019.04.201](https://doi.org/10.1016/j.conbuildmat.2019.04.201)
- Ilic M, Cheeseman C, Sollars C, Knight J. Mineralogy and microstructure of sintered lignite coal fly ash. *Fuel*. 2003;82:331–336. doi:[10.1016/S0016-2361\(02\)00272-7](https://doi.org/10.1016/S0016-2361(02)00272-7)
- Tishmack JK, Olek J, Diamond S, Sahu S. Characterization of pore solutions expressed from high-calcium fly-ash-water pastes. *Fuel*. 2001;80:815–819. doi:[10.1016/S0016-2361\(00\)00160-5](https://doi.org/10.1016/S0016-2361(00)00160-5)
- Sharonova OM, Anshits NN, Fedorchak MA, Zhizhaev AM, Anshits AG. Characterization of ferrospheres recovered from high-calcium fly ash. *Energy Fuels*. 2015;29:5404–5414. doi:[10.1021/acs.energyfuels.5b01618](https://doi.org/10.1021/acs.energyfuels.5b01618)
- Sharonova OM, Yumashev VV, Solovyov LA, Anshits AG. The fine high-calcium fly ash as the basis of composite cementing material. *Mag Civ Eng*. 2019;91:60–72. doi:[10.18720/MCE.91.6](https://doi.org/10.18720/MCE.91.6)
- Li Z. *Advanced concrete technology*. John Wiley & Sons, Inc: New Jersey, USA; 2011. 506 p <https://pdf.pub/advanced-concrete-technology.html>
- Yoshioka K, Tazawa EI, Kawai K, Enohata T. Adsorption characteristics of superplasticizers on cement component minerals. *Cem Concr Res*. 2002;32:1507–1513. doi:[10.1016/S0008-8846\(02\)00782-2](https://doi.org/10.1016/S0008-8846(02)00782-2)
- Alonso MM, Palacios M, Puertas F. Compatibility between polycarboxylate-based admixtures and blended-cement pastes. *Cem Concr Compos*. 2013;35:151–162. doi:[10.1016/j.cemconcomp.2012.08.020](https://doi.org/10.1016/j.cemconcomp.2012.08.020)
- Solovyov LA. Full-profile refinement by derivative difference minimization research papers. *J Appl Crystallogr*. 2004;37:743–749. doi:[10.1107/S0021889804015638](https://doi.org/10.1107/S0021889804015638)
- Fomenko EV, Yumashev VV, Kukhtetskiy SV, Zhizhaev AM, Anshits AG. Scanning electron microscopy-energy-dispersive X-ray spectrometry (SEM-EDS) analysis of PM<sub>1-2</sub> microspheres located in coal char particles with different morphologies. *Energy Fuels*. 2020;34:8848–8856. doi:[10.1021/acs.energyfuels.0c01345](https://doi.org/10.1021/acs.energyfuels.0c01345)

20. Lothenbach B, Scrivener K, Hooton RD. Supplementary cementitious materials. *Cem Concr Res.* 2011;41:1244–1256. doi:[10.1016/j.cemconres.2010.12.001](https://doi.org/10.1016/j.cemconres.2010.12.001)
21. Yu J, Lu C, Leung CKY, Li G. Mechanical properties of green structural concrete with ultrahigh-volume fly ash. *Constr Build Mater.* 2017;147:510–518. doi:[10.1016/j.conbuildmat.2017.04.188](https://doi.org/10.1016/j.conbuildmat.2017.04.188)
22. Durdziński PT, Dunant CF, Haha MB, Scrivener KL. A new quantification method based on SEM-EDS to assess fly ash composition and study the reaction of its individual components in hydrating cement paste. *Cem Concr Res.* 2015;73:111–122. doi:[10.1016/j.cemconres.2015.02.008](https://doi.org/10.1016/j.cemconres.2015.02.008)
23. Fediuk R, Timokhin R, Mochalov A, Otsokov K, Lashina I. Performance properties of high-density impermeable cementitious paste. *J Mater Civ Eng.* 2019;31:04019013. doi:[10.1061/\(asce\)mt.1943-5533.0002633](https://doi.org/10.1061/(asce)mt.1943-5533.0002633)
24. Ferrari L, Kaufmann J, Winnefeld F, Plank J. Multi-method approach to study influence of superplasticizers on cement suspensions. *Cem Concr Res.* 2011;41:1058–1066. doi:[10.1016/j.cemconres.2011.06.010](https://doi.org/10.1016/j.cemconres.2011.06.010)
25. Yang J, Su Y, He X, Tan H, Jiang Y, Zeng L, Strnadel B. Pore structure evaluation of cementing composites blended with coal by-products: Calcined coal gangue and coal fly ash. *Fuel Process Technol.* 2018;181:75–90. doi:[10.1016/j.fuproc.2018.09.013](https://doi.org/10.1016/j.fuproc.2018.09.013)